

# Exchange Processes in Shibasaki's Rare Earth Alkali Metal BINOLate Frameworks and Their Relevance in Multifunctional Asymmetric Catalysis

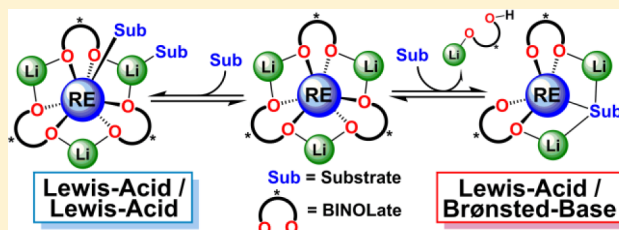
Jerome R. Robinson, Jun Gu, Patrick J. Carroll, Eric J. Schelter,\* and Patrick J. Walsh\*

P. Roy and Diana T. Vagelos Laboratories, Department of Chemistry, University of Pennsylvania, Philadelphia, Pennsylvania 19104, United States

## Supporting Information

**ABSTRACT:** Shibasaki's rare earth alkali metal BINOLate (REMB) catalysts (REMB; RE = Sc, Y, La – Lu; M = Li, Na, K; B = 1,1-bi-2-naphtholate; RE/M/B = 1/3/3) are among the most successful enantioselective catalysts and have been employed in a broad range of mechanistically diverse reactions. Despite the phenomenal success of these catalysts, several fundamental questions central to their reactivity remain unresolved. Combined reactivity and spectroscopic studies were undertaken to probe the identity of the active catalyst(s)

in Lewis-acid (LA) and Lewis-acid/Brønsted-base (LA/BB) catalyzed reactions. Exchange spectroscopy provided a method to obtain rates of ligand and alkali metal self-exchange in the RE/Li frameworks, demonstrating the utility of this technique for probing solution dynamics of REMB catalysts. Isolation of the first crystallographically characterized REMB complex with substrate bound enabled stoichiometric and catalytic reactivity studies, wherein we observed that substrate deprotonation by the catalyst framework was necessary to achieve selectivity. Our spectroscopic observations in LA/BB catalysis are inconsistent with previous mechanistic proposals, which considered only tris(BINOLate) species as active catalysts. These findings significantly expand our understanding of the catalyst structure in these privileged multifunctional frameworks and identify new directions for development of new catalysts.



## 1. INTRODUCTION

Rare-earth complexes continue to find great utility in asymmetric catalysis,<sup>1</sup> with Shibasaki's rare-earth-alkali-metal heterobimetallic complexes,  $[M_3(THF)_n][(\text{BINOLate})_3\text{RE}]$  (REMB; RE = Sc, Y, La–Lu; M = Li (1–RE), Na (2–RE), K (3–RE); B = 1,1'-bi-2-naphtholate; RE/M/B = 1/3/3; Figure 1) among the most enantioselective and broadly applicable catalysts to date.<sup>1f,g,2</sup> A key attribute of this system is the diverse reactivity and selectivity achieved through choice of  $\text{RE}^{3+}$  and alkali metal.<sup>2a,b,3</sup> Despite the remarkable reactivity and selectivity of these heterobimetallics, our understanding of these catalysts remains underdeveloped.<sup>3b,c,4</sup> Significant ad-

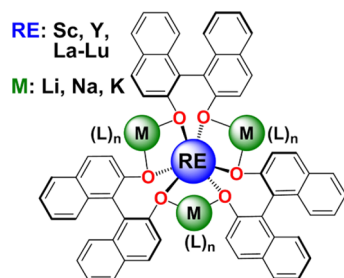


**Figure 1.** Shibasaki's REMB framework. RE = Sc, Y, La – Lu; M = Li, Na, K; B = (S)-BINOLate; RE/M/B = 1/3/3.

vancements have been made with regard to the solid state and solution characterization of  $[M_3(\text{THF})_n][(\text{BINOLate})_3\text{RE}]$  complexes, which are the proposed species that enter the catalytic cycles.<sup>3b,4a–k</sup> The identities and structures of the active catalyst *in operando*, however, remain largely unknown, leaving several fundamental questions unresolved. These include the following: (1) Do the BINOLate ligands or alkali-metal cations,  $M^+$ , undergo intra- or intermolecular exchange during catalysis and are these processes catalytically relevant? (2) Do the BINOLate ligands dissociate in the presence of protic substrates to generate metal complexes with less than three BINOLate ligands coordinated? (3) What are the active species generated during catalysis? Answers to these questions are critical to our understanding of these and other multifunctional catalysts and are necessary for the rational design of improved catalysts.

To date, the reaction in which the structure of the active REMB catalyst has been most thoroughly investigated was the Lewis-acid/Lewis-acid (LA/LA) catalyzed aza-Michael addition of *O*-methylhydroxylamine to chalcone derivatives.<sup>3b,4k,5</sup> In this case, a combination of NMR spectroscopy and rate studies were used to characterize the likely active catalyst structure. Conversely, almost nothing is known about the active catalyst

Received: March 4, 2015

Published: May 12, 2015

structure in Lewis-acid/Bronsted-base (LA/BB) catalyzed reactions, despite LA/BB reactions constituting the vast majority (>90%) of reported REMB catalyzed reactions.<sup>1g,2a–d,3c–h</sup> Mass spectrometry has been commonly used to interrogate the structure of REMB frameworks, however, these measurements do not provide definitive structural information due to the propensity of the ionic species of interest to undergo fragmentation even under mild ionization conditions.<sup>2a,b,3c,e,g,i,4l</sup> Essential qualitative and quantitative information regarding elementary catalytic reaction steps, such as substrate deprotonation and ligand- and/or cation-exchange, have not been determined, which greatly limits the assessment of viable catalytic species and cycles. As such, there is a critical need to apply new spectroscopic techniques to study active species in REMB asymmetric catalysis to contribute to our understanding of this important system.

Herein we report combined spectroscopic and mechanistic investigations of the RE/Li frameworks to uncover attributes of the active catalysts in Lewis-acid/Lewis-acid (LA/LA) and Lewis-acid/Bronsted-base (LA/BB) catalyzed reactions. 2D NMR exchange spectroscopy (EXSY) was determined to be a powerful technique for the study of these systems. Rates and activation parameters of intermolecular self-exchange involving BINOLate ligands and Li<sup>+</sup> cations were determined using EXSY and found to occur rapidly under catalytically relevant conditions. Our key findings are that the associative nature of these processes disfavor proposals of BINOLate dissociation to form coordinatively unsaturated *bis*(BINOLate) intermediates, [Li<sub>n</sub>(L)<sub>n</sub>][(BINOLate)<sub>2</sub>RE(L)<sub>n</sub>] (L = solvent or substrate), as catalytically active species in LA/LA catalyzed reactions.

In contrast, under LA/BB conditions, completely different catalyst structures were observed from those in the LA/LA catalyzed reactions. Isolation of the first crystallographically characterized example of a REMB complex with substrate bound enabled stoichiometric and catalytic reactivity studies, wherein we observed that substrate deprotonation by the catalyst framework was necessary to achieve selectivity. The dissociation of Li(BINOLate) was observed spectroscopically, in coordinating solvent, for both nonselective (Michael) and selective (Henry) reaction conditions. The formation of *bis*(BINOLate) catalytic intermediates was implicated in those cases. Our spectroscopic observations stand in contrast to the basic assumptions made in previous mechanistic proposals, which considered that only *tris*(BINOLate) species were involved during catalysis and redefines our understanding of the catalyst structure in these important multifunctional frameworks.

## 2. RESULTS AND DISCUSSION

**2.1. BINOLate and Li<sup>+</sup> Intermolecular Self-Exchange and Implications in Lewis-Acid/Lewis-Acid (LA/LA) Catalysis.** Independently, Shibasaki<sup>2b,3b</sup> and Salvadori<sup>4b,j</sup> determined that intermolecular BINOL and BINOLate ligand exchange processes occurred in select instances for REMB frameworks. Shibasaki and co-workers demonstrated through <sup>1</sup>H NMR spectroscopy and observation of pronounced nonlinear effects, that the heterochiral and homochiral diastereomers, 1-Y(het) and 1-Y(homo), respectively, underwent facile intermolecular BINOLate ligand exchange under catalytically relevant conditions. Although insightful for the origin of nonlinear effects in the aza-Michael reaction, the study did not attempt to quantify rates of ligand exchange. Using saturation transfer NMR experiments and near-Infrared circular

dichroism (NIR-CD), Salvadori and co-workers observed intermolecular BINOLate/BINOL ligand exchange between 3-Yb and free (R)- or (S)-BINOL. However, due to the poor spectral resolution in the exchange experiments, ligand exchange rates were only obtained in the case of 3-Yb(RRR) with (R)-BINOL. Notably, even less is known about the solution lability of M<sup>+</sup> in these heterobimetallic frameworks,<sup>6</sup> despite their implication in the regulation of substrate activation and catalyst structure.<sup>2b,d,3a,c,4l</sup> As such, we set out to apply a method that would observe and quantify intermolecular BINOLate and Li<sup>+</sup> exchange in 1-RE complexes.

We postulated that intermolecular BINOLate and M<sup>+</sup> exchange processes for [Li<sub>3</sub>(THF)<sub>4</sub>][(BINOLate)<sub>3</sub>RE(THF)]·THF (1-RE) could be observed using two-dimensional exchange spectroscopy (2D EXSY)<sup>7</sup> using <sup>1</sup>H- and <sup>7</sup>Li NMR. 2D EXSY NMR has emerged as a powerful tool to determine rates of chemical exchange in a number of diverse systems,<sup>7b,8</sup> including Li<sup>+</sup> exchange in solution<sup>9</sup> and solid states.<sup>10</sup> Application of this technique requires that sufficient spectral resolution is achieved between analytes of interest.<sup>7b,d</sup> To accomplish the requisite resolution for the study of 1-RE, we labeled otherwise chemically identical compounds by using two different paramagnetic RE<sup>3+</sup> cations. Pr and Eu cations were chosen because the 1-Pr and 1-Eu complexes are isostructural,<sup>4e</sup> and have desirable NMR spectroscopic properties including relatively long relaxation times and paramagnetic induced chemical shifts of opposite signs.<sup>11</sup>

Effectively equimolar mixtures of 1-Pr and 1-Eu in THF-*d*<sub>8</sub> displayed well-resolved <sup>1</sup>H and <sup>7</sup>Li NMR spectra corresponding to the two heterobimetallic frameworks. <sup>1</sup>H and <sup>7</sup>Li 2D EXSY NMR experiments were performed at 300 K using several mixing times, *t*<sub>mix</sub> (see Supporting Information). Appreciable rates of intermolecular exchange of both Li<sup>+</sup> cations (20.5 s<sup>-1</sup>) and BINOLate ligands (0.759 s<sup>-1</sup>) were observed (Figures 2, 3, and Table 1).

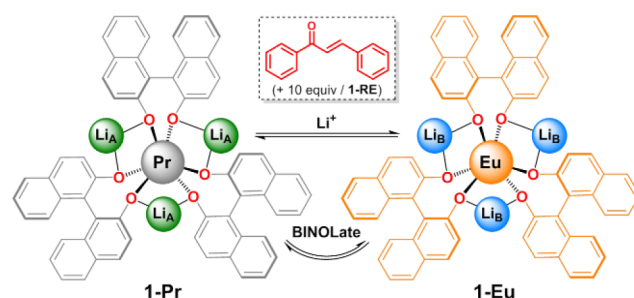


**Figure 2.** Intermolecular exchange observed by <sup>1</sup>H and <sup>7</sup>Li 2D EXSY NMR experiments. Bound solvents not shown for clarity.

Notably, Li<sup>+</sup> cation exchange occurred ~27 times faster between 1-Pr and 1-Eu than BINOLate exchange, indicative that Li<sup>+</sup> exchange was not coupled to BINOLate exchange. Activation parameters for BINOLate and Li<sup>+</sup> exchange were calculated using EXSYCalc<sup>12</sup> from variable temperature data collected between 273–330 K (Table 1, Figure S23 and S25). Both exchange processes displayed large positive enthalpies of activation and large negative entropies of activation (Table 1), consistent with associative processes.<sup>13</sup>

After obtaining rates for intermolecular BINOLate and Li<sup>+</sup> cation exchange, we were interested in establishing the relevance of these processes to catalysis. The first reaction we interrogated was the LA/LA mediated aza-Michael additions

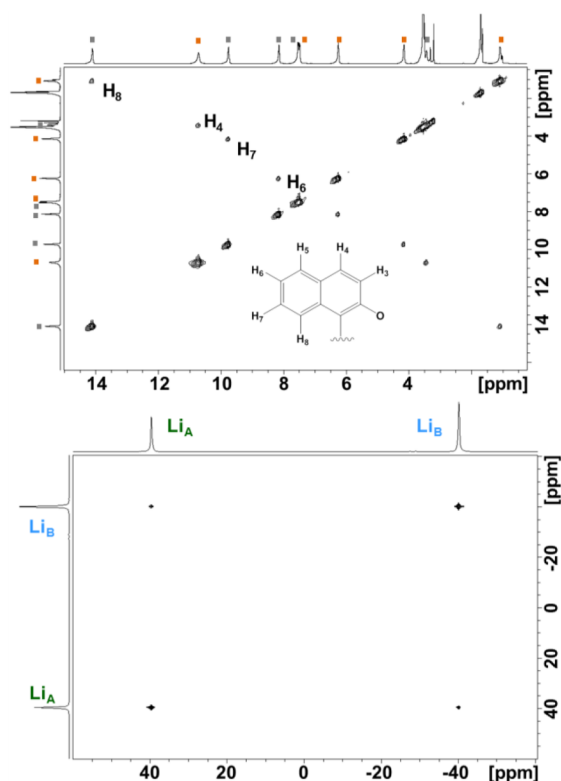
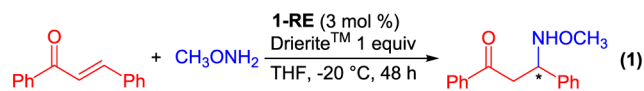


**Figure 3.** Representative 2D EXSY NMR spectra recorded for the mixture of **1-Pr**/**1-Eu** (13.1/14.6 mM) in THF-*d*<sub>8</sub> at 300 K observing: (A) <sup>1</sup>H NMR (400 MHz, *t*<sub>mix</sub> = 140 ms); grey ■ = **1-Pr**, orange ■ = **1-Eu** and (B) <sup>7</sup>Li NMR (126 MHz, *t*<sub>mix</sub> = 10 ms) Li<sub>A</sub> = **1-Pr**, Li<sub>B</sub> = **1-Eu**.

reaction (eq 1).<sup>3b,4k,5</sup> Reaction kinetics and spectroscopic studies for the LA/LA catalyzed aza-Michael addition were



previously reported, allowing for direct comparison of exchange processes to relevant reaction data. Several key findings from the previous studies were that (1) the reaction showed a first order dependence on chalcone and catalyst and a zero order dependence on *O*-methylhydroxylamine; (2) **1-RE** (RE = La – Dy, Y) catalyzed the reaction with comparable rates and selectivities; (3) the reaction rate was uninhibited by addition of Li<sub>2</sub>(BINOLate).<sup>3b,4k</sup>

Addition of 10 equiv of chalcone per **1-RE** produced negligible differences in BINOLate and Li<sup>+</sup> self-exchange rates

in EXSY experiments, and activation parameters for self-exchange were nearly identical to those obtained in the absence of chalcone (Table 1). The extrapolated pseudo-first-order rate constant for the BINOLate self-exchange process at the catalytically relevant reaction temperature, –20 °C, was  $7.5 \times 10^{-3} \text{ s}^{-1}$  ( $\nu = 1.1 \times 10^{-4} \text{ M s}^{-1}$ ). BINOLate and Li<sup>+</sup> self-exchange proceeded at 10<sup>2</sup>–10<sup>3</sup>-fold faster rates than the reported catalytic reaction,  $\nu = 2.8 \times 10^{-6} \text{ M s}^{-1}$ ,<sup>3b,4k,5</sup> which indicated that these exchange processes were not rate determining in catalysis and occurred with high frequency.

Notably, the activation parameters of the exchange processes speak directly to viable catalytic intermediates. Formation of proposed *bis*(BINOLate) RE species, [Li<sub>*x*</sub>(L)<sub>*n*</sub>], [(BINOLate)<sub>2</sub>RE(L)<sub>*n*</sub>] (L = substrate or solvent, *x* = 1 or 2), would require a dissociative BINOLate exchange, however, the self-exchange processes we observed were associative in nature. Similar conclusions disfavoring the possibility of BINOLate dissociation were reached from the previous kinetics study where the reaction rate of the aza-Michael reaction was found to be uninhibited upon addition of 1–3 mol % Li<sub>2</sub>(BINOLate) when using 1 mol % **1-Y** as a catalyst.<sup>4k</sup> Therefore, we propose that the active species under LA or LA/LA catalysis<sup>2b,3,4b,14</sup> would be substrate and solvent bound **1-RE** (Figure 4), sharing structural similarities to the recently reported solid state X-ray structures.<sup>4a,d,e,h,i,15</sup>

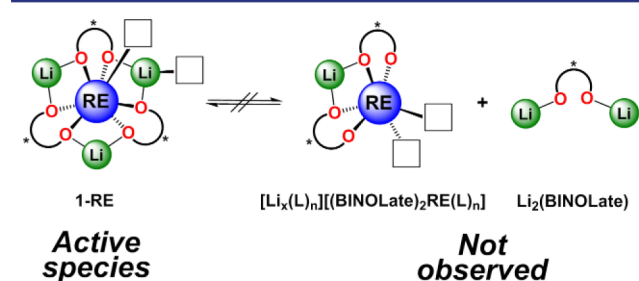


**Figure 4.** Proposed and observed catalytic species involved in the LA/LA catalyzed aza-Michael addition reaction. Boxes represent open coordination sites.

**2.2. Investigation of Active Species Generated under Lewis-Acid/Brønsted-Base (LA/BB) Catalysis.** The majority of reactions catalyzed by the REMB framework are Lewis-acid/Brønsted-base (LA/BB) mediated, wherein a basic BINOLate ligand deprotonates the pronucleophile to activate the substrate.<sup>1g,2b–d,3d–h,16</sup> Despite the predominance of this class of reactions, little is known about the active catalysts. Notably, it has not been determined whether BINOLate ligands undergo complete or partial ligand dissociation upon accepting a proton

**Table 1.** Associated EXSY Rate Data and Activation Parameters for **1-Pr**/**1-Eu**

exchange process	<i>k'</i> (s <sup>-1</sup> ) <sup>a</sup>	Δ <i>H</i> <sup>‡</sup> (kcal mol <sup>-1</sup> ) <sup>b</sup>	Δ <i>S</i> <sup>‡</sup> (eu) <sup>b</sup>	Δ <i>G</i> <sup>‡</sup> (kcal mol <sup>-1</sup> ) <sup>b</sup>
<b>1-Pr</b> → <b>1-Eu</b>				
Li <sup>+</sup> <sup>d</sup>	20.5 (20.7) <sup>c</sup>	8.46 (7.73)	–101 (–111)	15.7 (15.7)
BINOLate <sup>e</sup>	0.759 (0.899) <sup>c</sup>	14.8 (13.8)	–39.3 (–51.7)	17.6 (17.5)
<b>1-Eu</b> → <b>1-Pr</b>				
Li <sup>+</sup> <sup>d</sup>	21.4 (22.3) <sup>c</sup>	8.49 (7.66)	–100 (–111)	15.6 (15.6)
BINOLate <sup>e</sup>	0.806 (1.03) <sup>c</sup>	14.5 (13.1)	–42.9 (–60.7)	17.6 (17.4)

<sup>a</sup>At 300 K, [1-Pr]/[1-Eu] = 15.0/14.6 mM. *k'* values determined using EXSYCalc. <sup>b</sup>At 298 K. <sup>c</sup>Values obtained in the presence of ~10 equiv of chalcone/1-RE. <sup>d</sup>Values obtained at *t*<sub>mix</sub> = 7.5 ms. Additional *t*<sub>mix</sub> at 300 K can be found in Table S5. <sup>e</sup>Values obtained from H<sub>8</sub> at *t*<sub>mix</sub> = 140 ms. Additional values for H<sub>4</sub> and H<sub>7</sub> along with other *t*<sub>mix</sub> at 300 K can be found in Tables S1–S3.



from the pronucleophile (Figure 5). It has been proposed that RE complexes are coordinated by three BINOLate ligands

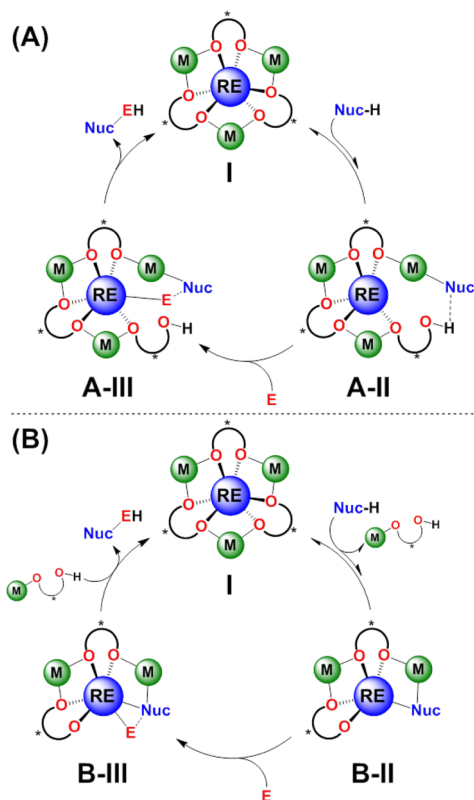
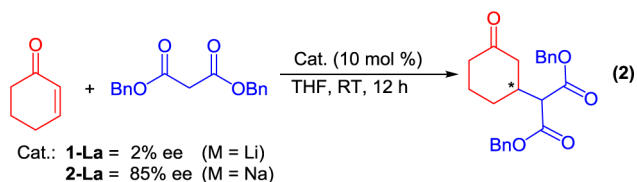


**Figure 5.** Proposed catalytic cycles of REMB (I) catalyzed LA/BB reactions involving monomeric active species (A) RE/M/B = 1:3:3,<sup>1g,2b,d,3d,i,16,17</sup> and (B) RE/M/B = 1:2:2.<sup>4g,j</sup>

throughout LA/BB catalytic cycles, regardless of the pronucleophile or RE/M combination used (Figure 5, A).<sup>1g,2b,d,3d,i,16,17</sup> BINOLate ligand dissociation and exchange for nucleophiles has been implicated by Salvadori and co-workers (Figure 5, B),<sup>4g,j</sup> but there has been a shortage of solution-phase evidence under catalytic conditions to support these claims. To provide insight into the structure of the active catalysts, we investigated two mechanistically distinct LA/BB promoted transformations, the Michael and Henry reactions<sup>1g,2a,b,d</sup>

**2.2.1. Investigation of the Michael Reaction Promoted by 1-RE.** We began our studies focused on the enantioselective Michael addition of malonates to cyclic enones (eq 2).<sup>2b</sup> 1-RE



(M = Li) are often the most enantioselective catalysts of the REMB frameworks; however, this particular Michael addition is a notable exception. Use of 10 mol % 1-La (M = Li) in THF reportedly produced Michael adducts between cyclohexenone (CHO) and dibenzylmalonate (DBM) in poor selectivity (2% ee), whereas 2-La (M = Na) showed high selectivity (85% ee).<sup>2b</sup> These differences in selectivity were not readily explained

by solution binding studies, which indicated that 1-RE binds CHO at the RE<sup>3+</sup> cation more readily than 2-RE. Additional structural information could inform on these subtleties, however, to date crystallographic characterization of an REMB framework with a substrate bound has proven elusive. As such, we initiated our studies by isolating a substrate-bound example, facilitated by our recent isolation of seven-coordinate RE-neutral donor adducts.<sup>4a,d,e,h,i,15</sup>

Successful isolation of the first substrate-bound REMB complex, [Li<sub>3</sub>(THF)(Et<sub>2</sub>O)<sub>2</sub>(CHO)][(BINOLate)<sub>3</sub>Pr(CHO)] (1-Pr<sup>2</sup>CHO, Figure 6), was accomplished by treating 1-Pr

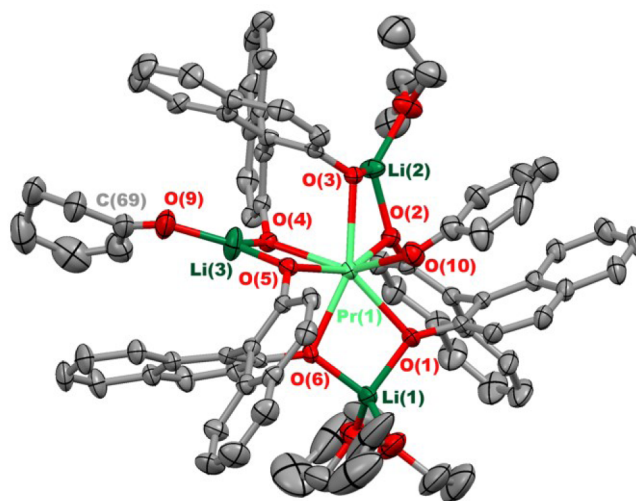


**Figure 6.** Thermal ellipsoid plot of 1-Pr<sup>2</sup>CHO projected at the 30% probability level. Selected bond distances (Å): Pr(1)-O(1) 2.403(2), Pr(1)-O(2) 2.404(2), Pr(1)-O(3) 2.4603(18), Pr(1)-O(4) 2.414(2), Pr(1)-O(5) 2.365(2), Pr(1)-O(6) 2.3683(18), Pr(1)-O(10) 2.525(2), Li(3)-O(9) 1.872(6), C(69)-O(9) 1.232(5), and C(75)-O(10) 1.221(4).

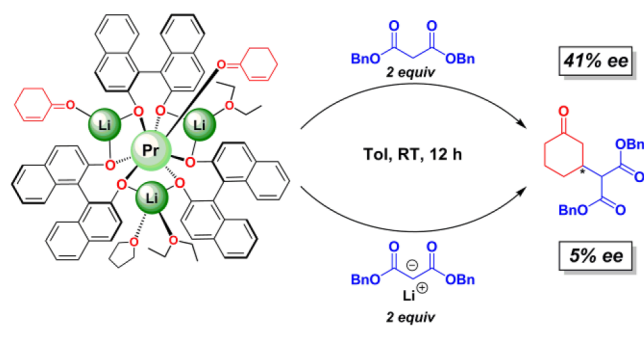
with  $\geq 4$  equiv CHO in diethyl ether solution followed by layering with pentane (1:2 v/v; 86% crystalline yield). The use of weakly coordinating solvent was critical for the isolation of 1-Pr<sup>2</sup>CHO; attempts to crystallize substrate bound examples of RE/M combinations: RE = La, Pr; M = Li, Na, K using THF as the solvent resulted in isolation of only the THF bound REMB compounds.<sup>17</sup>

1-Pr<sup>2</sup>CHO included two molecules of coordinated CHO; one CHO was bound at the Pr<sup>3+</sup> cation while the other bound at a Li<sup>+</sup> cation. The bonding metrics for 1-Pr<sup>2</sup>CHO were consistent with related Pr<sup>3+</sup>/Li<sup>+</sup> REMB structures,<sup>4a,d,15</sup> and the observed Lewis-base coordination at both Pr<sup>3+</sup> and Li<sup>+</sup> cations was similar to the recently reported phosphine oxide adducts.<sup>4h</sup> Dissolving crystals of 1-Pr<sup>2</sup>CHO in the noncoordinating solvent toluene-*d*<sub>8</sub> revealed exchange of CHO between the Pr<sup>3+</sup> and three Li<sup>+</sup> sites. Exchange was fast on the NMR time-scale, as evidenced by a single <sup>7</sup>Li NMR resonance and two alkenyl resonances in the <sup>1</sup>H NMR spectra (Figure S3d,e). Consistent with previous binding studies,<sup>2b,4a,d</sup> the use of the coordinating solvent THF-*d*<sub>8</sub> resulted in competitive coordination of THF with CHO at the RE<sup>3+</sup> and Li<sup>+</sup> cations (Figure S3a-c).

**Stoichiometric and Catalytic Reaction Studies.** To establish the species generated under LA/BB mediated reaction conditions we first investigated the stoichiometric and catalytic reactivity of 1-Pr<sup>2</sup>CHO with dibenzylmalonate (DBM). We initiated our reactivity studies with 1-Pr<sup>2</sup>CHO in toluene-*d*<sub>8</sub>,

as the substrate would not be displaced by competitive coordination of the NMR solvent. Despite our observation that CHO rapidly exchanged between  $\text{Pr}^{3+}$  and  $\text{Li}^+$  cations in toluene- $d_8$  at room temperature, CHO was bound to a chiral Lewis acid in either environment (Figure S26). We postulated that addition of the preformed nucleophile,  $\text{DBM}^-$ , would proceed with moderate levels of enantioselectivity (Scheme 1).

**Scheme 1. Stoichiometric Reactivity of 1-Pr-2CHO with Dibenzylmalonate (DBM, Pronucleophile) or Lithium Dibenzylmalonate (Li(DBM), Preformed (External) Nucleophile)**



To our surprise, addition of two equiv Li(DBM) to 1-Pr-2CHO in toluene formed the product, 3-[bis-(benzyloxycarbonyl)methyl]cyclohexenone, with only low levels of enantiopurity (5% ee). In contrast, treatment of 1-Pr-2CHO with 2 equiv of the pronucleophile, DBM, formed the Michael adduct in 41% ee.

The observed reactivity and selectivity clearly demonstrated the multifunctional nature of the REMB catalysts. Simple LA coordination of the substrate does not provide an effective chiral environment for a highly enantioselective conjugate addition between an externally preformed malonate nucleophile to the coordinated substrate, CHO. The pronucleophile must be deprotonated by the catalyst to proceed selectively, and implies that the active catalyst structure is different than that found in 1-Pr-2CHO.

Solvent choice is often an important parameter to optimize catalyst performance for the REMB frameworks. Shibasaki and co-workers observed high levels of enantioselectivity in the Michael reaction using noncoordinating solvent ( $\text{CH}_2\text{Cl}_2$  and toluene) and low enantioselectivities using coordinating solvent (THF).<sup>2b,3f,16c</sup> They proposed that noncoordinating solvent disfavored formation of nonselective charge-separated salts. However, no spectroscopic evidence was provided to support these proposals. Considering these observations along with our previous binding studies, we hypothesized that catalytic reactions performed in THF would show lower levels of enantioselectivity due to preferential and competitive coordination of solvent at the RE cation.

Use of 10 mol % of either 1-Pr or 1-Pr-2CHO in toluene furnished active species of identical selectivities, where the catalytic reaction proceeded with diminished levels of enantioselectivity compared to the stoichiometric reaction (25% versus 40% ee). Under rigorously anhydrous conditions, use of 10 mol % 1-Pr or 1-Pr-2CHO as a catalyst in THF solvent resulted in a complete reversal in enantioselectivity, where Michael adducts were furnished in -25% ee. While the enantioselectivities obtained were low, the unexpected reversal in catalyst facial selectivity suggested a change in structure

associated with solvent choice and prompted further spectroscopic investigation of salient reaction conditions.<sup>18</sup>

**Spectroscopic Studies.** Insight into the identity of the active catalyst was provided by 1D and 2D  $^1\text{H}$  and  $^7\text{Li}$  NMR spectroscopies. As depicted in the two mechanistic proposals shown in Figure 5, addition of the pronucleophile, DBM, to 1-Pr would be expected to result in a deprotonation event, where either  $\text{DBM}^-$  and BINOLate ligands could remain tightly associated to form either six- or seven-coordinate RE complexes (Figure 5, A), or  $\text{DBM}^-$  could exchange with one equiv of coordinated Li(BINOLate) (Figure 5, B). We postulated that  $^7\text{Li}$  NMR resonances sensitized by a paramagnetic  $\text{RE}^{3+}$  cation, namely  $\text{Pr}^{3+}$ , would allow elimination of one of these mechanistic scenarios. Dissociated Li(BINOLate) would be easily found in the diamagnetic region of the  $^7\text{Li}$  NMR spectrum, while lithium cations proximate to the  $\text{Pr}^{3+}$  cation within an REMB framework would be expected to show significant paramagnetic shifts.<sup>15</sup>

Both stoichiometric and catalytic (10 mol %) reactions performed in toluene- $d_8$  solutions promoted by 1-Pr or 1-Pr-2CHO revealed the formation of new  $\text{Pr}^{3+}/\text{Li}^+$  heterobimetallic species together with a large amount of unreacted 1-Pr, as determined by  $^7\text{Li}$  NMR (Figures S15 and S16). The formation of the new  $\text{Pr}^{3+}/\text{Li}^+$  heterobimetallic species was found to be reversible. Several broadened paramagnetic resonances were observed upon addition of DBM, however, at reaction completion 1-Pr was the only observable paramagnetic species (Figures S16 and S17).

A key observation was that neither free external nucleophile, Li(DBM), nor completely dissociated monolithiated BINOLate ligand, Li(BINOLate), were observed by  $^7\text{Li}$  NMR during the course of either the stoichiometric or catalytic reactions performed in toluene. The absence of Li(DBM) or Li(BINOLate) formed during the reaction was consistent with a structurally intact complex formed upon deprotonation of DBM with 1-Pr. The absence of the diamagnetic  $^7\text{Li}$  signals of Li(BINOLate) and Li(DBM) could be due to excessive line broadening associated with fast-exchange of these  $\text{Li}^+$  species with  $\text{Pr}/\text{Li}^+$  species. However, the spectroscopic observations were further corroborated by independent control experiments. Use of 10 mol % Li(BINOLate) or Li(DBM) effectively promoted racemic background reactions at comparable rates to 1-Pr. Given these observations, the possibility of forming large amounts of either Li(BINOLate) or Li(DBM) during the reaction is unlikely, as Michael adducts from stoichiometric and catalytic conditions were formed with moderate levels of enantioselectivity. Therefore, we favor a proposed catalytic cycle similar to that shown in Figure 5A.

In contrast, a different scenario was observed for the catalytic reaction performed in THF- $d_8$ . Addition of 10 equiv of DBM to either 1-Pr or 1-Pr/CHO (1:10) resulted in a complex  $^1\text{H}$  NMR spectra with many new paramagnetic signals (Figures S9, S11, and S14). The resulting  $^7\text{Li}$  NMR spectra of the catalytic reaction proved more informative (Figure 7, B); it consisted of three major species,  $\text{Li}_A$ ,  $\text{Li}_B$ , and  $\text{Li}_C$  (67% of the total Li present), along with ~six minor signals ( $\text{Li}_D$ - $\text{Li}_J$ ; 33% of the total Li present). Notably, the relative concentration and number of resonances observed in the  $^7\text{Li}$  NMR spectra were dependent on the concentration of 1-Pr and DBM, where under the catalytically relevant concentrations  $\text{Li}_A$ ,  $\text{Li}_B$ , and  $\text{Li}_C$  were formed in a ~1:1.1:0.5 ratio, and 11 other paramagnetic Li signals were observed (Figure S35). Upon addition of CHO the spectrum simplified to that displayed in Figure 7B (top).  $^1\text{H}$

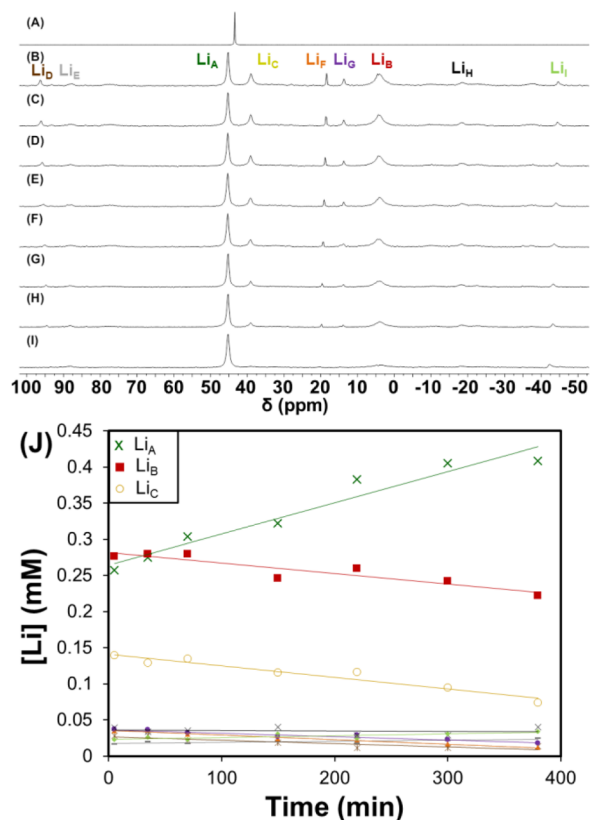


**Figure 7.**  $^7\text{Li}$  NMR spectra (155 MHz,  $\text{THF-}d_6$ ) taken of the catalytic Michael reaction promoted by **1-Pr** (41.7 mM, 10 mol %) at various % conversion (A) **1-Pr** (B) < 5% (C) 15% (D) 24% (E) 36% (F) 48% (G) 59% (H) 65%, (I) 95%. (J) Concentration of  $\text{Li}_A$  (green  $\times$ , **1-Pr**),  $\text{Li}_B$  (red  $\blacksquare$ ,  $\text{Li}(\text{BINOLate})$ ),  $\text{Li}_C$  (brown  $\circ$ , **4-Pr**) and  $\text{Li}_D$ – $\text{Li}_I$  from 0 to ~65% conversion of the catalytic Michael addition between CHO and DBM promoted by 10 mol % **1-Pr** (41.7 mM) in THF as determined by  $^7\text{Li}$  NMR. Lines are provided as guides for the eye.

and  $^7\text{Li}$  spectroscopy indicated that the new heterobimetallic species formed reversibly, as **1-Pr** was regenerated as the sole observable paramagnetic signal at the conclusion of the catalytic reaction (Figure 7, I (top)).

Located near 40 ppm in the  $^7\text{Li}$  NMR spectrum (Figure 7, B),  $\text{Li}_A$  was definitively assigned as **1-Pr** (25%). A diamagnetic resonance,  $\text{Li}_B$ , was assigned as a rapidly exchanging mixture of  $\text{Li}(\text{BINOLate})$  and  $\text{Li}(\text{DBM})$ , which was established through independent preparation and spectroscopic analysis of  $\text{Li}(\text{DBM})$  and  $\text{Li}_n(\text{BINOLate})$  ( $n = 1$  and  $2$ ; Figure S10). Observation of dissociated  $\text{Li}(\text{BINOLate})$  requires the formation of at least one new RE heterobimetallic species with less than three coordinated BINOLate ligands (Figure 8).

Consistent with this conclusion, monitoring the addition of varying equivalents of DBM to **1-Pr** by  $^1\text{H}$  and  $^7\text{Li}$  NMR spectroscopy revealed consumption of **1-Pr** concomitant with growth of  $\text{Li}_B$  and the major paramagnetic product,  $\text{Li}_C$  (Figure S9). High concentrations of DBM resulted in the growth of six additional minor Li signals ( $\text{Li}_D$  –  $\text{Li}_I$ ), consistent with these species originating from an acid–base equilibrium between **1-Pr** and DBM. Accordingly, we have tentatively assigned  $\text{Li}_C$ , the major  $\text{Pr}^{3+}/\text{Li}^+$  heterobimetallic complex, as either  $[\text{Li}_2(\text{sol})][(\text{BINOLate})_2\text{Pr}(\text{DBM})]$ , **4-Pr**, or more likely, oligomers containing the  $[\text{Li}_2(\text{sol})][(\text{BINOLate})_2\text{Pr}(\text{DBM})]$  moiety. We propose that the remaining six  $^7\text{Li}$  signals ( $\text{Li}_D$  –  $\text{Li}_I$ ; Figure 7,

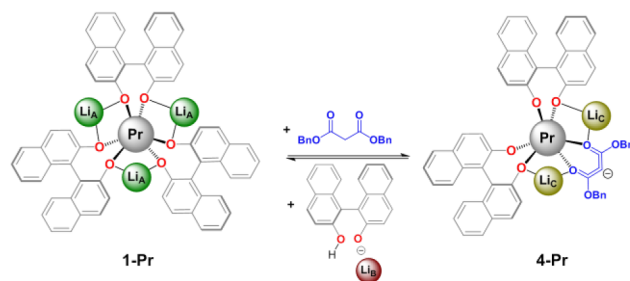


**Figure 8.** Major exchange processes and proposed species observed by 2D  $^7\text{Li}$  NMR EXSY experiment of **1-Pr**/DBM (45.5 mM/455 mM;  $t_{\text{mix}} = 15$  ms, 300 K). Bound solvents not shown.

B) to be products formed from further deprotonation and ligand exchange between  $\text{Li}_C$  and additional DBM or oligomeric species with less than three BINOLate ligands per Pr cation. Another key spectroscopic observation supportive of our assignment of  $\text{Li}_C$  and  $\text{Li}_D$ – $\text{Li}_I$  was the ratio of  $\text{Li}_B$ : $\text{Li}_C$ . If the reaction of **1-Pr** with DBM was the only source of  $\text{Li}(\text{BINOLate})/\text{Li}(\text{DBM})$ , then the expected ratio of  $\text{Li}_B$ : $\text{Li}_C$  would be 1:1. However, the observed 2:1 ratio was indicative that  $\text{Li}(\text{BINOLate})/\text{Li}(\text{DBM})$  was not solely generated from **1-Pr**.

NMR exchange experiments performed in THF provided additional information on the solution behavior of the catalyst, **1-Pr**. 2D  $^7\text{Li}$  EXSY NMR experiments performed on a solution of **1-Pr**/DBM (1:10) at 300 K (Figure 9) indicated

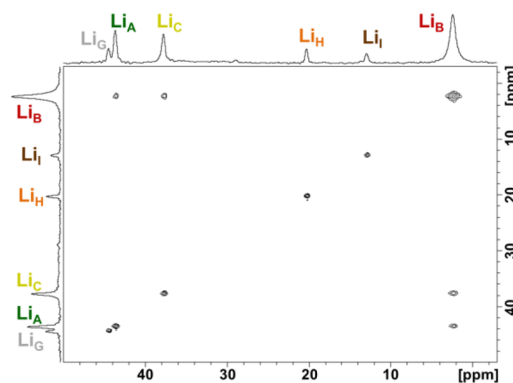


**Figure 9.** 2D  $^7\text{Li}$  NMR EXSY experiment of **1-Pr**/DBM (45.5 mM/455 mM;  $t_{\text{mix}} = 15$  ms, 300 K).

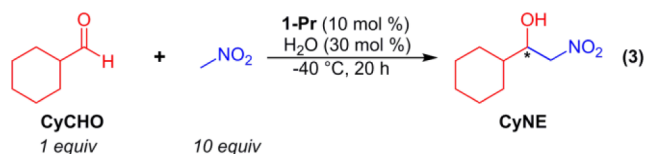
that  $\text{Li}_A$ ,  $\text{Li}_B$ , and  $\text{Li}_C$  underwent facile exchange with one another at rates ( $k' = 5$ – $55$   $\text{s}^{-1}$ ) comparable to the intermolecular exchange observed between **1-Pr**/**1-Eu** (Table S10).<sup>19</sup> Reversible ligand-exchange and deprotonation was further corroborated through the use of 2D  $^1\text{H}$  EXSY NMR spectroscopy. Exchange cross-peaks were observed for **1-Pr**,  $\text{Li}(\text{BINOLate})$ , DBM, and additional unidentified paramagnetic species. Because of spectral overlap, analysis of exchange rates was not possible (Figure S33).

The results of our reactivity and spectroscopic studies provide data to revise previously proposed catalytic cycles and modes of action for **1-RE** in catalysis. Our isolation of the first crystallographically characterized example of a REMB framework with bound substrate enabled stoichiometric and catalytic studies probing the identity of the active catalyst. Stoichiometric reactions performed in toluene demonstrated the multifunctional nature of **1-Pr**, where selectivity was only achieved when the active nucleophile was generated upon



deprotonation by **1-Pr**. Choice of coordinating or non-coordinating solvent favored distinctly different species during catalysis. In toluene, dissociation of Li(BINOLate) was not observed, which was consistent with previously proposed catalytic cycles such as the one shown in Figure 5A. In THF, reaction of **1-Pr** and DBM resulted in the reversible dissociation Li(BINOLate), as observed by 1D and 2D NMR spectroscopy. These results were consistent with a catalytic cycle similar to Figure 5B. While the observation of Li(BINOLate) indirectly implied the formation of REMB complexes with less than three coordinated BINOLate ligands during the reaction, the definitive structural identification of the active catalyst will require further mechanistic studies.

**2.2.2. Investigation of the Henry Reaction promoted by 1-Pr.** During our study of the Michael addition reaction we were intrigued that **1-Pr** was a highly selective catalyst for the Henry and Aldol reactions, but showed poor selectivity in the Michael reaction. We hypothesized that the observed selectivity differences could be related to the acidity of the pronucleophile. In Shibasaki's seminal reports on the reactivity of chiral RE alkoxides, poor selectivities and complete exchange of substrate for ligand were observed using more acidic substrates.<sup>2d</sup> Similarly, our spectroscopic results on the acidic malonate pronucleophile,  $pK_a$  15.9–16.4 in DMSO,<sup>20</sup> indicated that ligand exchange for substrate occurred, resulting in a diverse Pr/Li speciation. With these results in mind, we hypothesized that the less acidic nitromethane,  $pK_a$  17.2 in DMSO,<sup>21</sup> or acetophenone,  $pK_a$  24.7 in DMSO,<sup>21</sup> substrates would undergo deprotonation less readily, minimizing the concentration of off-cycle, less selective Pr/Li species. To test our hypothesis, we turned our attention to the catalytic enantioselective Henry reaction (eq 3).



The catalytic Henry reaction between 1 equiv cyclohexanecarboxaldehyde (CyCHO) and 10 equiv nitromethane using 10 mol % **1-Pr** and 30 mol % water<sup>22</sup> at  $-40\text{ }^\circ\text{C}$  (233 K) in THF or THF- $d_8$  furnished (*R*)-1-cyclohexyl-2-nitroethanol (CyNE) with similar yields and selectivity (95% yield, 90% ee) as the original report (eq 3).<sup>2a,23</sup> Unlike the Michael reaction and consistent with our hypothesis, introduction of the less acidic pronucleophile, nitromethane, initially generated little Li(BINOLate) or other Pr/Li species (Figure 10, B). The consumption of **1-Pr** and CyCHO showed a zero order rate dependence (Figure 11, A), suggesting catalyst saturation was operative under the reaction conditions.

Additional insight into the catalytic intermediates formed in the Henry reaction was gained by monitoring the reaction using  $^7\text{Li}$  NMR (Figure 10, A–H, and Figure 11 B). While the consumption of **1-Pr** was a zero order process, the kinetics associated with the formation of additional Pr/Li and Li-containing species was more complex. Five additional Li resonances grew in over the course of the reaction ( $\text{Li}_A$ – $\text{Li}_F$ ), where again  $\text{Li}_A$  corresponded to unreacted **1-Pr** and  $\text{Li}_B$  was Li(BINOLate). While the new heterobimetallic species could not be definitively assigned, the rates and relative integrations of  $\text{Li}_C$ – $\text{Li}_F$  (Figure 11, B) are informative in identifying the

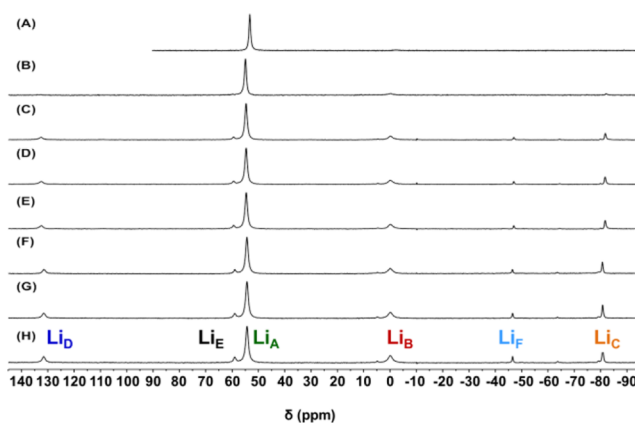


**Figure 10.**  $^7\text{Li}$  NMR spectra (155 MHz, THF- $d_8$ ) taken of the catalytic Henry reaction promoted by **1-Pr** (24.6 mM, 10 mol %) at various % conversion (A) **1-Pr** + CyCHO +  $\text{H}_2\text{O}$  (B) +  $\text{CH}_3\text{NO}_2$  (10 equiv); <1% (C) 7% (D) 12% (E) 19% (F) 22% (G) 32% (H) 37% conversion.  $\text{Li}_A = \text{1-Pr}$ ;  $\text{Li}_B = \text{Li(BINOLate)}$ .

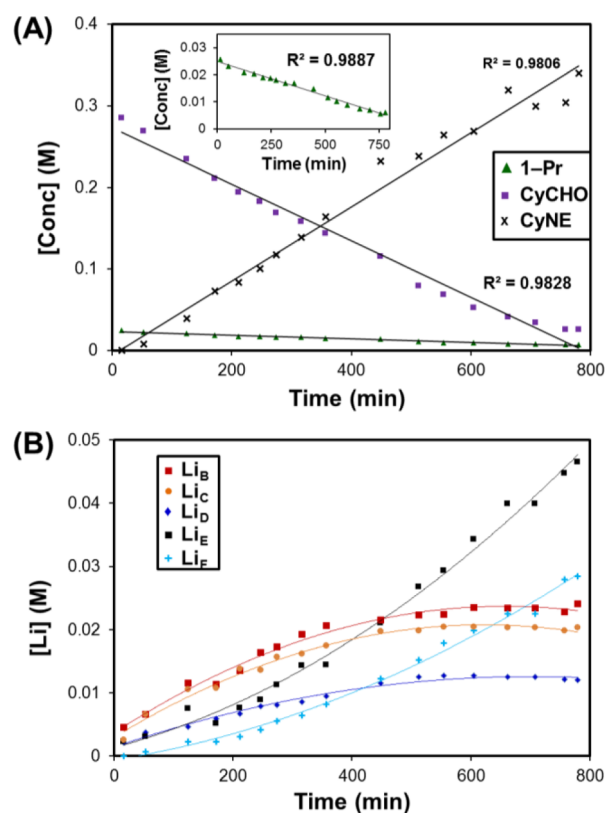


**Figure 11.** (A) Concentration of **1-Pr** (green  $\blacktriangle$ ), cyclohexylcarboxaldehyde (CyCHO, purple  $\blacksquare$ ), and (*R*)-1-cyclohexyl-2-nitroethanol (CyNE, black  $\times$ ) over the course of the catalytic Henry reaction by **1-Pr** (24.6 mM, 10 mol %) as determined by  $^1\text{H}$  NMR. Inset centered on **1-Pr**.  $R^2$  values presented next to linear fit. (B) Concentration of  $\text{Li}_B$  (red  $\blacksquare$ ; Li(BINOLate)),  $\text{Li}_C$  (orange  $\bullet$ ),  $\text{Li}_D$  (blue  $\blacklozenge$ ),  $\text{Li}_E$  (black  $\blacksquare$ ), and  $\text{Li}_F$  (cyan  $+$ ) with respect to time. Lines provided as guides for the eye.

relevant species involved. There are two distinct processes which occur during catalysis; one is the reaction of **1-Pr** with  $\text{CH}_3\text{NO}_2$  to form Li(BINOLate),  $\text{Li}_C$ , and  $\text{Li}_D$ , while the other process involves the formation of another heterobimetallic species ( $\text{Li}_E$  and  $\text{Li}_F$ ) composed of chemically inequivalent  $\text{Li}^+$  centers in a 2:1 ratio. In order to provide further insight into

the species generated in the Henry reaction and how the substrates interact with the catalyst, we monitored the addition of varying equivalents of  $\text{CH}_3\text{NO}_2$  to **1-Pr** and **1-Pr**/CyCHO/ $\text{H}_2\text{O}$  at RT (Figures S21–S25).

Similar to the Michael reaction, increased concentration of pronucleophile resulted in the generation of new heterobimetallic species ( $\text{Li}_\text{C}$ ,  $\text{Li}_\text{D}$ , and  $\text{Li}_\text{E}$ ) and consumption of **1-Pr** (Figure S22).  $\text{Li}_\text{C}$  and  $\text{Li}_\text{D}$ , 94 and  $-42$  ppm respectively, were formed in a  $\sim 1:1$  ratio, whereas  $\text{Li}_\text{E}$ ,  $-25$  ppm, was only observable in trace amounts at the highest concentrations of  $\text{CH}_3\text{NO}_2$ . This was consistent with the higher  $\text{p}K_\text{a}$  of  $\text{CH}_3\text{NO}_2$ , which would require a larger excess of  $\text{CH}_3\text{NO}_2$  to generate deprotonated nucleophile. At RT,  $\text{Li}^+$  cation exchange was fast on the NMR time scale for the catalytic Henry reaction, and the characteristic diamagnetic Li signal associated with Li(BINOLate) was not observed.

The presence of water can have a large effect on the stereoselectivity of REMB catalyzed reactions, yet the role of water is not always well understood.  $^1\text{H}$  NMR spectra recorded after the addition of  $\text{H}_2\text{O}$  (30 mol %) to **1-Pr** (10 mol %) indicated coordination of  $\text{H}_2\text{O}$  to the  $\text{Pr}^{3+}$  cation, even in the presence of one equiv CyCHO (Figure S21). While reversible coordination of  $\text{H}_2\text{O}$  to the  $\text{RE}^{3+}$  in the REMB framework has been demonstrated in the solid state and solution,<sup>2a,3b,4e,k,5</sup> the result was surprising given the strong preference of aldehyde coordination to a RE cation observed in previous anhydrous binding studies.<sup>4a,d</sup> Evidence for decomposition of **1-RE** at higher  $\text{H}_2\text{O}$  levels ( $>10$  equiv relative to **1-RE**) has been demonstrated,<sup>1x</sup> however, decomposition of the catalyst is unlikely under the conditions investigated for the Henry reaction.

Monitoring the catalytic reaction at RT performed with 1 equiv  $\text{CH}_3\text{NO}_2$  provided additional insight into substrate catalyst interactions. The heterobimetallic species generated from addition of  $\text{CH}_3\text{NO}_2$  to **1-Pr**,  $\text{Li}_\text{C}$  and  $\text{Li}_\text{D}$ , were not observed when only one equiv  $\text{CH}_3\text{NO}_2$  was used. On the other hand, addition of 10 equiv of  $\text{CH}_3\text{NO}_2$  resulted in an initial build-up followed by rapid consumption of  $\text{Li}_\text{C}$  and  $\text{Li}_\text{D}$ , consistent with their involvement as active species in catalysis (Figure S24, B). Unlike the use of 10 equiv  $\text{CH}_3\text{NO}_2$ , only  $\sim 85\%$  conversion could be attained using one equiv of  $\text{CH}_3\text{NO}_2$  (Figure S23c). This observation suggests that free/excess  $\text{CH}_3\text{NO}_2$  is needed for turnover. Additionally, the other heterobimetallic species,  $\text{Li}_\text{E}$ , appears to build up with excess  $\text{CH}_3\text{NO}_2$  without CyCHO to react with, and could likely represent an off-cycle process.

In accordance with the observations from our spectroscopic studies, we propose that the catalytic Henry reaction follows a catalytic cycle similar to that found in Figure 5B. Evidence for the dissociation of Li(BINOLate) was found under catalytic conditions for the Henry reaction along with the addition of varying equivalents of  $\text{CH}_3\text{NO}_2$  to **1-Pr**. We propose that  $\text{Li}_\text{C}/\text{Li}_\text{D}$  belong to the active heterobimetallic species, which is formed from the reaction of **1-Pr** with  $\text{CH}_3\text{NO}_2$ . While additional investigation into the structure of the catalytic intermediates is needed and will be the topic of future study, our results clearly indicated that ligand exchange between substrate and BINOLate occurs during the course of the highly enantioselective Henry reaction.

### 3. CONCLUSIONS

Shibasaki's REMB frameworks are among the most enantioselective catalysts discovered to date. However, 20 years after

their initial discovery their mechanism of action is still not understood. We have established through 2D EXSY NMR studies that both  $\text{Li}^+$  cations and BINOLate ligands undergo self-exchange at much faster rates than that of catalytic reactions. For LA and LA/LA catalysis these self-exchange processes are associative in nature, and exclude *bis*(BINOLate) species as active intermediates in these catalytic cycles.

On the other hand in the presence of an acidic pronucleophile, as is the case during LA/BB catalysis, a different mechanistic scenario was operative. Our isolation of the first crystallographically characterized REMB framework with a substrate coordinated enabled stoichiometric reactivity studies, which indicated that selectivity was only observed when the nucleophile was generated through deprotonation by **1-Pr**. Use of coordinating solvent favored the dissociation of Li(BINOLate) during catalysis, which was observed in both the catalytic Michael and Henry reactions. Exchange between **1-Pr**, Li(BINOLate), and putative *bis*(BINOLate) species, **4-Pr**, occurred readily at RT with DBM as the pronucleophile. The implication of **4-Pr** calls previous mechanistic proposals for involvement of only the tris(BINOLate) species in catalytic cycles (Figure 5, A) into question. Our studies have shown that *bis*(BINOLate) or oligomeric heterobimetallic species of this moiety are likely candidates for catalytically active species, and that the active species generated will likely vary significantly depending on the solvent and nucleophile used. Our results clearly indicate that these reactions are more mechanistically complex than originally assumed, and illustrate the need for further structural and mechanistic studies to ascertain the true identity of the active catalysts.

### ■ ASSOCIATED CONTENT

#### 📄 Supporting Information

Experimental details, NMR spectra, SFC chromatograms of racemic and enantioenriched product, and crystallographic data (CIF). The Supporting Information is available free of charge on the ACS Publications website at DOI: 10.1021/jacs.5b02201.

### ■ AUTHOR INFORMATION

#### Corresponding Authors

\*schelter@sas.upenn.edu

\*pwalsh@sas.upenn.edu

#### Notes

The authors declare no competing financial interest.

### ■ ACKNOWLEDGMENTS

E.J.S. and P.J.W. acknowledge the University of Pennsylvania and the NSF (CHE-1026553 and CHE-0840438 for an X-ray diffractometer) for financial support of this work.

### ■ REFERENCES

- (1) Recent reviews: (a) Matsunaga, S.; Shibasaki, M. *Chem. Commun.* **2014**, *50*, 1044–1057. (b) Averill, D. J.; Allen, M. J. *Catal. Sci. Technol.* **2014**, *4*, 4129–4137. (c) Deng, Q.-H.; Melen, R. L.; Gade, L. H. *Acc. Chem. Res.* **2014**, *47*, 3162–3173. (d) Kitanosono, T.; Kobayashi, S. *Adv. Synth. Catal.* **2013**, *355*, 3095–3118. (e) Ward, B. D.; Gade, L. H. *Chem. Commun.* **2012**, *48*, 10587–10599. (f) Park, J.; Hong, S. *Chem. Soc. Rev.* **2012**, *41*, 6931–6943. (g) Shibasaki, M.; Kanai, M.; Matsunaga, S.; Kumagai, N. *Acc. Chem. Res.* **2009**, *42*, 1117–1127. Recent publications (2014–2015): (h) Li, W.; Tan, F.; Hao, X.; Wang, G.; Tang, Y.; Liu, X.; Lin, L.; Feng, X. *Angew. Chem., Int. Ed.* **2015**, *54*, 1608–1611. (i) Xiao, X.; Mei, H.; Chen, Q.; Zhao, X.; Lin, L.; Liu, X.;



- Feng, X. *Chem. Commun.* **2015**, *51*, 580–583. (j) Cao, W.; Liu, X.; Guo, J.; Lin, L.; Feng, X. *Chem.—Eur. J.* **2015**, *21*, 1632–1636. (k) Xia, Y.; Liu, X.; Zheng, H.; Lin, L.; Feng, X. *Angew. Chem., Int. Ed.* **2015**, *54*, 227–230. (l) Hashimoto, K.; Kumagai, N.; Shibasaki, M. *Chem.—Eur. J.* **2015**, *21*, 4262–4266. (m) Hashimoto, K.; Kumagai, N.; Shibasaki, M. *Org. Lett.* **2014**, *16*, 3496–3499. (n) Tamura, K.; Kumagai, N.; Shibasaki, M. *J. Org. Chem.* **2014**, *79*, 3272–3278. (o) Maudoux, N.; Roisnel, T.; Carpentier, J.-F.; Sarazin, Y. *Organometallics* **2014**, *33*, 5740–5748. (p) Wang, Z.; Yao, Q.; Kang, T.; Feng, J.; Liu, X.; Lin, L.; Feng, X. *Chem. Commun.* **2014**, *50*, 4918–4920. (q) Song, G.; O, W. W. N.; Hou, Z. *J. Am. Chem. Soc.* **2014**, *136*, 12209–12212. (r) Qian, Q.; Tan, Y.; Zhao, B.; Feng, T.; Shen, Q.; Yao, Y. *Org. Lett.* **2014**, *16*, 4516–4519. (s) Chen, W.; Lin, L.; Cai, Y.; Xia, Y.; Cao, W.; Liu, X.; Feng, X. *Chem. Commun.* **2014**, *50*, 2161–2163. (t) Bai, S.; Liao, Y.; Lin, L.; Luo, W.; Liu, X.; Feng, X. *J. Org. Chem.* **2014**, *79*, 10662–10668. (u) Zhou, L.; Liu, X.; Ji, J.; Zhang, Y.; Wu, W.; Liu, Y.; Lin, L.; Feng, X. *Org. Lett.* **2014**, *16*, 3938–3941. (v) Chu, Y.; Hao, X.; Lin, L.; Chen, W.; Li, W.; Tan, F.; Liu, X.; Feng, X. *Adv. Synth. Catal.* **2014**, *356*, 2214–2218. (w) Hao, X.; Liu, X.; Li, W.; Tan, F.; Chu, Y.; Zhao, X.; Lin, L.; Feng, X. *Org. Lett.* **2014**, *16*, 134–137. (x) Robinson, J. R.; Fan, X.; Yadav, J.; Carroll, P. J.; Wooten, A. J.; Pericàs, M. A.; Schelter, E. J.; Walsh, P. J. *J. Am. Chem. Soc.* **2014**, *136*, 8034–8041. (y) Robinson, J. R.; Yadav, J.; Fan, X.; Stanton, G. R.; Schelter, E. J.; Pericàs, M. A.; Walsh, P. J. *Adv. Synth. Catal.* **2014**, *356*, 1243–1254.
- (2) (a) Sasai, H.; Suzuki, T.; Itoh, N.; Tanaka, K.; Date, T.; Okamura, K.; Shibasaki, M. *J. Am. Chem. Soc.* **1993**, *115*, 10372–10373. (b) Sasai, H.; Arai, T.; Satow, Y.; Houk, K. N.; Shibasaki, M. *J. Am. Chem. Soc.* **1995**, *117*, 6194–6198. (c) Shibasaki, M.; Yoshikawa, N. *Chem. Rev.* **2002**, *102*, 2187–2209. (d) Shibasaki, M.; Sasai, H.; Arai, T. *Angew. Chem., Int. Ed.* **1997**, *36*, 1237–1256. (e) Walsh, P. J.; Kozlowski, M. C. *Fundamentals of Asymmetric Catalysis*; University Science Books: Sausalito, CA, 2008; p 674.
- (3) (a) Sone, T.; Yamaguchi, A.; Matsunaga, S.; Shibasaki, M. *J. Am. Chem. Soc.* **2008**, *130*, 10078–10079. (b) Yamagiwa, N.; Qin, H. B.; Matsunaga, S.; Shibasaki, M. *J. Am. Chem. Soc.* **2005**, *127*, 13419–13427. (c) Yamagiwa, N.; Tian, J.; Matsunaga, S.; Shibasaki, M. *J. Am. Chem. Soc.* **2005**, *127*, 3413–3422. (d) Schlemminger, I.; Saida, Y.; Groger, H.; Maison, W.; Durot, N.; Sasai, H.; Shibasaki, M.; Martens, J. *J. Org. Chem.* **2000**, *65*, 4818–4825. (e) Yoshikawa, N.; Yamada, Y. M. A.; Das, J.; Sasai, H.; Shibasaki, M. *J. Am. Chem. Soc.* **1999**, *121*, 4168–4178. (f) Emori, E.; Arai, T.; Sasai, H.; Shibasaki, M. *J. Am. Chem. Soc.* **1998**, *120*, 4043–4044. (g) Groger, H.; Saida, Y.; Sasai, H.; Yamaguchi, K.; Martens, J.; Shibasaki, M. *J. Am. Chem. Soc.* **1998**, *120*, 3089–3103. (h) Sasai, H.; Arai, T.; Sahara, Y.; Shibasaki, M. *J. Org. Chem.* **1995**, *60*, 6656–6657. (i) Arai, T.; Yamada, Y. M. A.; Yamamoto, N.; Sasai, H.; Shibasaki, M. *Chem.—Eur. J.* **1996**, *2*, 1368–1372.
- (4) (a) Wooten, A. J.; Carroll, P. J.; Walsh, P. J. *J. Am. Chem. Soc.* **2008**, *130*, 7407–7419. (b) Wooten, A. J.; Salvi, L.; Carroll, P. J.; Walsh, P. J. *Adv. Synth. Catal.* **2007**, *349*, 561–565. (c) Wooten, A. J.; Carroll, P. J.; Walsh, P. J. *Org. Lett.* **2007**, *9*, 3359–3362. (d) Wooten, A. J.; Carroll, P. J.; Walsh, P. J. *Angew. Chem., Int. Ed.* **2006**, *45*, 2549–2552. (e) Aspinall, H. C.; Bickley, J. F.; Dwyer, J. L. M.; Greeves, N.; Kelly, R. V.; Steiner, A. *Organometallics* **2000**, *19*, 5416–5423. (f) Aspinall, H. C.; Dwyer, J. L. M.; Greeves, N.; Steiner, A. *Organometallics* **1999**, *18*, 1366–1368. (g) Di Bari, L.; Lelli, M.; Pintacuda, G.; Pescitelli, G.; Marchetti, F.; Salvadori, P. *J. Am. Chem. Soc.* **2003**, *125*, 5549–5558. (h) Robinson, J. R.; Gordon, Z.; Booth, C. H.; Carroll, P. J.; Walsh, P. J.; Schelter, E. J. *J. Am. Chem. Soc.* **2013**, *135*, 19016–19024. (i) Robinson, J. R.; Carroll, P. J.; Walsh, P. J.; Schelter, E. J. *Angew. Chem., Int. Ed.* **2012**, *51*, 10159–10163. (j) Di Bari, L.; Lelli, M.; Salvadori, P. *Chem.—Eur. J.* **2004**, *10*, 4594–4598. (k) Yamagiwa, N.; Matsunaga, S.; Shibasaki, M. *Angew. Chem., Int. Ed.* **2004**, *43*, 4493–4497. (l) Horiuchi, Y.; Gnanadesikan, V.; Ohshima, T.; Masu, H.; Katagiri, K.; Sei, Y.; Yamaguchi, K.; Shibasaki, M. *Chem.—Eur. J.* **2005**, *11*, 5195–5204.
- (5) Yamagiwa, N.; Matsunaga, S.; Shibasaki, M. *J. Am. Chem. Soc.* **2003**, *125*, 16178–16179.
- (6) Previous solution characterization has been limited to mass spectrometry. See refs 2b, d, 3e, 4l.
- (7) (a) Orrell, K. G., *Two-Dimensional Methods of Monitoring Exchange*. In *eMagRes*; John Wiley & Sons, Ltd: New York, NY, 2007. (b) Perrin, C. L.; Dwyer, T. J. *Chem. Rev.* **1990**, *90*, 935–967. (c) Jeener, J.; Meier, B. H.; Bachmann, P.; Ernst, R. R. *J. Chem. Phys.* **1979**, *71*, 4546–4553; (d) *Coord. Chem. Rev.* **1996**, *150*, 185–220.
- (8) (a) Babailov, S. P. *Prog. Nucl. Magn. Reson. Spectrosc.* **2008**, *52*, 1–21. (b) Cahill, L. S.; Chapman, R. P.; Britten, J. F.; Goward, G. R. *J. Phys. Chem. B* **2006**, *110*, 7171–7177. (c) Pastor, A.; Martinez-Viviente, E. *Coord. Chem. Rev.* **2008**, *252*, 2314–2345. (d) Kalverda, A. P.; Salgado, J.; Dennison, C.; Canters, G. W. *Biochemistry* **1996**, *35*, 3085–3092. (e) Fischer, S.; Grootenhuus, P. D. J.; Groenen, L. C.; Vanhooft, W. P.; Vanveggel, F.; Reinhoudt, D. N.; Karplus, M. *J. Am. Chem. Soc.* **1995**, *117*, 1611–1620. (f) Chen, M. C.; Roberts, J. A. S.; Marks, T. J. *J. Am. Chem. Soc.* **2004**, *126*, 4605–4625. (g) Brotin, T.; Lesage, A.; Emsley, L.; Collet, A. *J. Am. Chem. Soc.* **2000**, *122*, 1171–1174. (h) Banci, L.; Bertini, I.; Briganti, F.; Luchinat, C.; Scozzafava, A.; Oliver, M. V. *Inorg. Chem.* **1991**, *30*, 4517–4524. (i) Dunand, F. A.; Aime, S.; Merbach, A. E. *J. Am. Chem. Soc.* **2000**, *122*, 1506–1512. (j) Aime, S.; Botta, M.; Ermondi, G. *Inorg. Chem.* **1992**, *31*, 4291–4299. (k) Willem, R. *Prog. Nucl. Magn. Reson. Spectrosc.* **1988**, *20*, 1–94. (l) Heise, J. D.; Raftery, D.; Breedlove, B. K.; Washington, J.; Kubiak, C. P. *Organometallics* **1998**, *17*, 4461–4468.
- (9) (a) Arvidsson, P. I.; Ahlberg, P.; Hilmersson, G. *Chem.—Eur. J.* **1999**, *5*, 1348–1354. (b) Hilmersson, G.; Malmros, B. *Chem.—Eur. J.* **2001**, *7*, 337–341. (c) Li, D. Y.; Sun, C. Z.; Williard, P. G. *J. Am. Chem. Soc.* **2008**, *130*, 11726–11736. (d) Pöppler, A.-C.; Meinhof, M. M.; Faßhuber, H.; Lange, A.; John, M.; Stalke, D. *Organometallics* **2011**, *31*, 42–45. (e) Bauer, W.; Feigl, M.; Mueller, G.; Schleyer, P. v. R. *J. Am. Chem. Soc.* **1988**, *110*, 6033–6046.
- (10) (a) Bottke, P.; Freude, D.; Wilkening, M. *J. Phys. Chem. C* **2013**, *117*, 8114–8119. (b) Davis, L. J. M.; Heinmaa, I.; Goward, G. R. *Chem. Mater.* **2009**, *22*, 769–775. (c) Cahill, L. S.; Chapman, R. P.; Britten, J. F.; Goward, G. R. *J. Phys. Chem. B* **2006**, *110*, 7171–7177. (d) Verhoeven, V. W. J.; de Schepper, I. M.; Nachtgeal, G.; Kentgens, A. P. M.; Kelder, E. M.; Schoonman, J.; Mulder, F. M. *Phys. Rev. Lett.* **2001**, *86*, 4314–4317. (e) Nagel, R.; Groß, T. W.; Günther, H.; Lutz, H. D. *Solid State Chem.* **2002**, *165*, 303–311.
- (11) (a) Cockerill, A. F.; Davies, G. L. O.; Harden, R. C.; Rackham, D. M. *Chem. Rev.* **1973**, *73*, 553–588. (b) Peters, J. A.; Huskens, J.; Raber, D. J. *Prog. Nucl. Magn. Reson. Spectrosc.* **1996**, *28*, 283–350.
- (12) Cobas, J. C.; Martin-Pastor, M. *EXSYCalc*, 1.0; Mestrelab Research: Santiago De Compostela, Spain.
- (13) (a) Jordan, R. B. *Reaction Mechanisms of Inorganic and Organometallic Systems*, 2nd ed.; Oxford University Press: New York, NY, 1998. (b) Asperger, S. *Chemical Kinetics and Inorganic Reaction Mechanisms*, 2nd ed.; Kluwer Academic: New York, NY, 2003.
- (14) Morita, T.; Arai, T.; Sasai, H.; Shibasaki, M. *Tetrahedron: Asymmetry* **1998**, *9*, 1445–1450.
- (15) Robinson, J. R.; Booth, C. H.; Carroll, P. J.; Walsh, P. J.; Schelter, E. J. *Chem.—Eur. J.* **2013**, *19*, 5996–6004.
- (16) (a) Tian, J.; Yamagiwa, N.; Matsunaga, S.; Shibasaki, M. *Angew. Chem., Int. Ed.* **2002**, *41*, 3636–3638. (b) Sasai, H.; Bougauchi, M.; Arai, T.; Shibasaki, M. *Tetrahedron Lett.* **1997**, *38*, 2717–2720. (c) Sasai, H.; Emori, E.; Arai, T.; Shibasaki, M. *Tetrahedron Lett.* **1996**, *37*, 5561–5564. (d) Sasai, H.; Tokunaga, T.; Watanabe, S.; Suzuki, T.; Itoh, N.; Shibasaki, M. *J. Org. Chem.* **1995**, *60*, 7388–7389. (e) Sasai, H.; Kim, W. S.; Suzuki, T.; Shibasaki, M.; Mitsuda, M.; Hasegawa, J.; Ohashi, T. *Tetrahedron Lett.* **1994**, *35*, 6123–6126.
- (17) While full characterization was only undertaken for **1-Pro2CHO**, other early RE's could also be readily crystallized using identical conditions.
- (18) It should be emphasized that the results of this Michael reaction were obtained under rigorously anhydrous conditions. The original work by Shibasaki and co-workers reported 2% ee for **1-La**; however, we have shown in a recent work (ref 1x) that trace amounts of water can have significant effects on the resulting stereoselectivity of the product.

(19) Exchange was also observed between two of the minor  $\text{Li}^+$  species,  $\text{Li}_D$  and  $\text{Li}_G$  (Figure S35 and Table S10). Absence of exchange of the remaining  $\text{Li}^+$  species was likely due to their shortened relaxation times.

(20) (a) Arnett, E. M.; Maroldo, S. G.; Schilling, S. L.; Harrelson, J. A. *J. Am. Chem. Soc.* **1984**, *106*, 6759–6767. (b) Olmstead, W. N.; Bordwell, F. G. *J. Org. Chem.* **1980**, *45*, 3299–3305.

(21) Matthews, W. S.; Bares, J. E.; Bartmess, J. E.; Bordwell, F. G.; Cornforth, F. J.; Drucker, G. E.; Margolin, Z.; McCallum, R. J.; McCollum, G. J.; Vanier, N. R. *J. Am. Chem. Soc.* **1975**, *97*, 7006–7014.

(22) 30 mol % of water was used to ensure the best reproducibility of observed catalyst performance. Previous reports introduced water either through the synthesis of the catalyst or as an additive, ranging from 30 to 1500 mol % (refs 2a, 3c, 23)

(23) Sasai, H.; Suzuki, T.; Itoh, N.; Arai, S.; Shibasaki, M. *Tetrahedron Lett.* **1993**, *34*, 2657–2660.